

# PHYS 350

## 3 Body Simulation

Don Nguyen (26748146),  
David Ma (19123141),  
Jason Lee (33462136),  
Tynan Stack (14400139),  
Winnie Mui (36278142)

April 19, 2017

### 1 Introduction

The three body problem has historical significance to humanity due to early attempts to model and predict the Earth, Moon, and Sun as three isolated bodies, interacting via gravity. However, as science advanced it was discovered that this was a dramatic oversimplification of the overall solar system. Even though the three body problem may not accurately describe the Earth-Moon-Sun system, it still has applications in a variety of important problems that can be modeled as three body systems such as triple star systems or when using certain assumptions for the Earth-Sun-Jupiter system. The goal of our project is to analyze the 3 body problem and build a simulation capable of modeling the problem given a variety of initial conditions. In order to do this, we analyzed the problem using Lagrangian and Hamiltonian mechanics, and utilized several integration methods to build a simulation of the derived equations of motion.

### 2 Derivation of Equations of Motion

#### 2.1 Basic Equations

For a three body system, the energy is:

$$E = T + V \quad (1)$$

where  $T$  is the kinetic energy

$$T = \sum_{i=1}^{N=3} \frac{1}{2} m_i \dot{\mathbf{r}}_i^2 \quad (2)$$

and  $V$  is the gravitational potential energy

$$V = -G \sum_{i < j} \frac{m_i m_j}{|\mathbf{r}_i - \mathbf{r}_j|} \quad (3)$$

in these equations  $m_i$  is the mass of one of the bodies,  $\dot{\mathbf{r}}_i = \frac{d\mathbf{r}_i}{dt}$  is the velocity of the bodies,  $G$  is the gravitational constant, and  $\mathbf{r}_i$  is the distance between the bodies.

#### 2.2 Lagrangian Equations

Lagrange's equations of motion are, for  $i = 1, 2, 3$ :

$$\frac{d}{dt} \left( \frac{\partial \mathcal{L}}{\partial \dot{\mathbf{r}}_i} \right) = \frac{\partial \mathcal{L}}{\partial \mathbf{r}_i} \quad (4)$$

Where  $\mathcal{L}$  denotes the Lagrangian:

$$\mathcal{L} = T - V \quad (5)$$

In our case, the Lagrangian is:

$$\mathcal{L} = \sum_{i=1}^{N=3} \frac{1}{2} m_i \dot{\mathbf{r}}_i^2 + G \sum_{i<j} \frac{m_i m_j}{|\mathbf{r}_i - \mathbf{r}_j|} \quad (6)$$

Taking the partial derivative with respect to  $\dot{\mathbf{r}}_i$  for  $i = 1, 2, 3$ :

$$\frac{\partial \mathcal{L}}{\partial \dot{\mathbf{r}}_i} = m_i \dot{\mathbf{r}}_i \quad (7)$$

Taking the time derivative:

$$\frac{d}{dt} \left( \frac{\partial \mathcal{L}}{\partial \dot{\mathbf{r}}_i} \right) = m_i \ddot{\mathbf{r}}_i \quad (8)$$

Taking the partial derivative with respect to  $\mathbf{r}_i$ :

$$\frac{\partial \mathcal{L}}{\partial \mathbf{r}_i} = -G \frac{\partial}{\partial \mathbf{r}_i} \left( \sum_{n<j} \frac{m_n m_j}{|\mathbf{r}_n - \mathbf{r}_j|} \right) = -G \sum_{\substack{j=1 \\ j \neq i}}^3 m_j \frac{\mathbf{r}_i - \mathbf{r}_j}{|\mathbf{r}_i - \mathbf{r}_j|^3} \quad (9)$$

Thus, Lagrange's equations of motion are, for  $i = 1, 2, 3$ :

$$\ddot{\mathbf{r}}_i = -G \sum_{\substack{j=1 \\ j \neq i}}^3 m_j \frac{\mathbf{r}_i - \mathbf{r}_j}{|\mathbf{r}_i - \mathbf{r}_j|^3} \quad (10)$$

## 2.3 Hamiltonian Equations

Canonical momentums are as follows for  $i = 1, 2, 3$ :

$$\mathbf{p}_{r_i} = \frac{\partial T}{\partial \dot{\mathbf{r}}_i} = m_i \dot{\mathbf{r}}_i \quad (11)$$

Hamiltonian's equations of motion are:

$$\mathcal{H} = \sum_{i=1}^{N=3} \frac{1}{2} \frac{\mathbf{p}_{r_i}^2}{m_i} - G \sum_{i<j} \frac{m_i m_j}{|\mathbf{r}_i - \mathbf{r}_j|} \quad (12)$$

To find the equations of motion, we find  $\dot{\mathbf{r}}_i$  and  $\dot{\mathbf{p}}_{r_i}$ :

$$\dot{\mathbf{r}}_i = \frac{\partial \mathcal{H}}{\partial \mathbf{p}_{r_i}} = \sum_{i=1}^{n=3} \frac{\mathbf{p}_{r_i}}{m_i} \quad (13)$$

$$\dot{\mathbf{p}}_{r_i} = -\frac{\partial \mathcal{H}}{\partial \mathbf{r}_i} = -G \sum_{i<j} \frac{m_i m_j}{|\mathbf{r}_i - \mathbf{r}_j|^2} \quad (14)$$

Finally, to get acceleration, we take the derivative of  $\dot{\mathbf{r}}_i$  with respect to time, and substitute in  $\dot{\mathbf{p}}_{r_i}$ :

$$\ddot{\mathbf{r}}_i = \sum_{i=1}^{n=3} \frac{\dot{\mathbf{p}}_i}{m_i} = -G \sum_{i=1}^{n=3} \sum_{i<j} \frac{m_i m_j}{m_i |\mathbf{r}_i - \mathbf{r}_j|^2} = -G \sum_{i=1}^{n=3} \sum_{i<j} \frac{m_j}{|\mathbf{r}_i - \mathbf{r}_j|^2} \quad (15)$$

## 2.4 Solutions

The second order equations that need to be solved are as follows:

$$\frac{d^2 \mathbf{r}_1}{dt^2} = -G m_2 \frac{\mathbf{r}_1 - \mathbf{r}_2}{|\mathbf{r}_1 - \mathbf{r}_2|^3} - G m_3 \frac{\mathbf{r}_1 - \mathbf{r}_3}{|\mathbf{r}_1 - \mathbf{r}_3|^3} \quad (16)$$

$$\frac{d^2 \mathbf{r}_2}{dt^2} = -G m_3 \frac{\mathbf{r}_2 - \mathbf{r}_3}{|\mathbf{r}_2 - \mathbf{r}_3|^3} - G m_1 \frac{\mathbf{r}_2 - \mathbf{r}_1}{|\mathbf{r}_2 - \mathbf{r}_1|^3} \quad (17)$$

$$\frac{d^2 \mathbf{r}_3}{dt^2} = -G m_1 \frac{\mathbf{r}_3 - \mathbf{r}_1}{|\mathbf{r}_3 - \mathbf{r}_1|^3} - G m_2 \frac{\mathbf{r}_3 - \mathbf{r}_2}{|\mathbf{r}_3 - \mathbf{r}_2|^3} \quad (18)$$

Since we are doing a 2-dimensional simulation, we only have 6 coupled second order equations (the 3 equations in the  $z$  direction are neglected). If we were to do a 3-dimensional simulation, we would have to solve 9 equations.

### 3 Known Analytical Solutions

There are currently 91 known analytical solutions to the 3 body gravitational problem. All of these solutions require extremely specific initial conditions and require renormalization of many parameters including, but not limited to, masses, the gravitational constant, velocities, and starting locations. Of the 17 known solutions only 5 will be discussed at length, however, a full list of the names of the solutions are:

- Broucke A (1-16)[[Bro75](#)]
- Broucke R (1-13)[[Bro75](#)]
- Henon (1-46) [[HEN76](#)] [[Hen74](#)]
- Figure 8 [[Moo93](#)][[CM00](#)]
- Butterfly (I,II,III,IV)[[SD13](#)]
- Bumblebee[[SD13](#)]
- Dragonfly[[SD13](#)]
- Goggles[[SD13](#)]
- Moth (I,II,III)[[SD13](#)]
- Yarn[[SD13](#)]
- Yin-Yang (1a,1b,2a,2b)

Before any of the solutions are discussed the conditions under which these solutions arise must be stated. These solutions will be broken up into 2 types: BROUCKE-HADJIDEMETRIOU-HENON (B-H-H) and everything else. The conditions for the B-H-H conditions follow: The initial conditions of these solutions are of the form  $(X_1,0),(X_2,0),(X_3,0)$  and velocities  $(0,\dot{Y}_1),(0,\dot{Y}_2),(0,\dot{Y}_3)$ , masses of bodies are  $1/3$ , and the HENON solutions are periodic up to a rotation through a certain angle. All of these solutions share a number of parameters:

- Gravitational constant is 1
- Movement is only considered in 2 dimensions
- Initial positions of the bodies are  $(-1,0),(1,0),(0,0)$  for bodies 1, 2, and 3 respectively
- Bodies all have mass 1

As a means of effectively displaying some of the solutions the state sphere representation will be used. The state sphere is a mathematical construct that used to effectively visualize interactions between the bodies. With red dots representing states that involve collisions between the bodies. Henceforth each orbit will be portrayed in whichever state space is most appropriate to its properties.

The first solution that will be shown explicitly is the Figure 8 solution. The Figure 8 solution<sup>1</sup> is the most simple orbit that will be discussed. The initial conditions for this solution are: Velocities:  $(p_1,p_2),(p_1,p_2),(-2p_1,-2p_2)$  for bodies 1, 2, and 3 respectively where  $p_1=0.347111$  and  $p_2=0.532728$ . This solution has total angular momentum of zero, and a period of approximately 6.3. This solution was found in 1993 by C. Moore [[Moo93](#)].

The second orbit that will be shown explicitly is the Goggles solution. The goggles solution<sup>2</sup> is significantly more complicated when compared to the figure 8 solution.

The name of this particular solution is more apparent when the solution is seen in shape sphere space<sup>3</sup> The state sphere representation is where the goggles solution got its name with the appearance of eyes on each side of the sphere and the over and under wrapping from the paths. The conditions for this solution are: Velocities  $(p_1,p_2),(p_1,p_2),(-2p_1,-2p_2)$  for bodies 1, 2, and 3 respectively where  $p_1=0.083300$ ,  $p_2=0.127889$ . The period is comparatively longer at 10.5 and angular momentum is once again zero. This solution along with the rest of the following solutions were discovered in 2012[[SD13](#)].

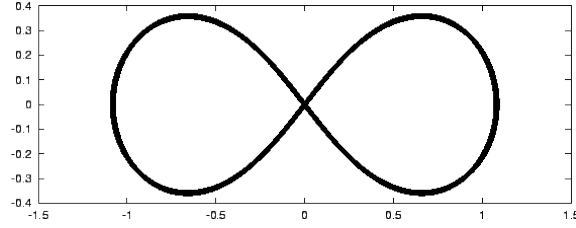


Figure 1: Figure 8 Solution

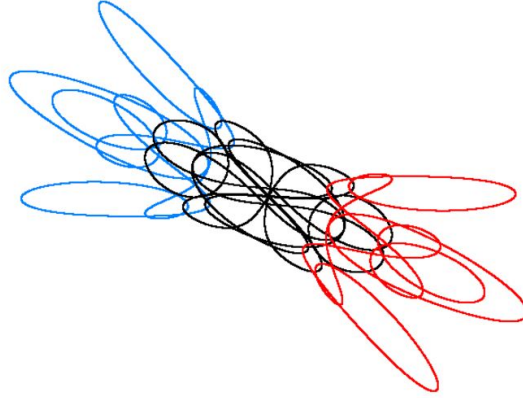


Figure 2: Goggles Solution

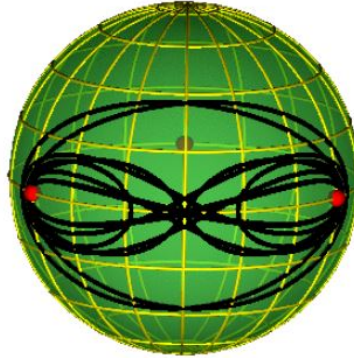


Figure 3: Goggles Solution Shape Sphere

The next solution is in the Yin-Yang group. This group contains 4 different orbits that share some common characteristics such as the appearance of their orbits to form a yin-yang type pattern in sphere space and generating intriguing paths in real space. For most of the families that are present in the solutions the shapes of the solutions are more or less the same with the most sparse solutions being the lower numbers and the most dense solutions being the higher numbers<sup>4</sup>.

This solution, unlike the Figure 8 or the Goggles solutions, does not have a mirror symmetry to it although there is still rotational symmetry. The conditions that establish this solution are: Velocities  $(p_1, p_2), (p_1, p_2), (-2p_1, -2p_2)$  for bodies 1, 2, and 3 respectively where  $p_1 = 0.416822$ ,  $p_2 = 0.330333$ . With a period significantly longer than the other two solutions discussed at 55.8 and angular momentum of zero.

The next solution also begins to a family called Moth which has three different solutions in the family. This family is named from a combination of the real space trace appearing similar to a moth and the sphere space tracing out somewhat of a flight pattern typical of a moth. The solution that will be shown is Moth III<sup>5,6</sup>.

This solution shares some properties with the Figure 8 and Goggles solutions such as having a mirror symmetry. Additionally the real space plot shares some visual similarities to the goggles solution. The conditions for this solutions are:  $(p_1, p_2), (p_1, p_2), (-2p_1, -2p_2)$  for bodies 1, 2, and

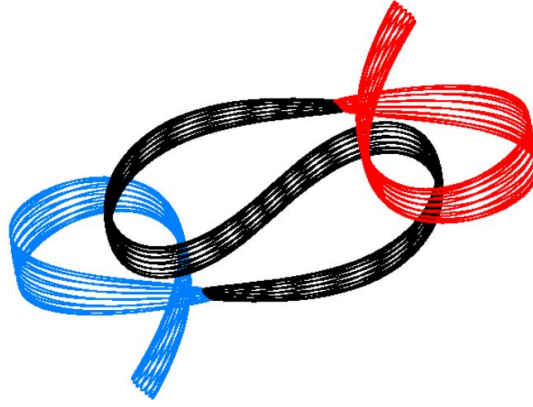


Figure 4: Yin-Yang 2a Real Space Solution

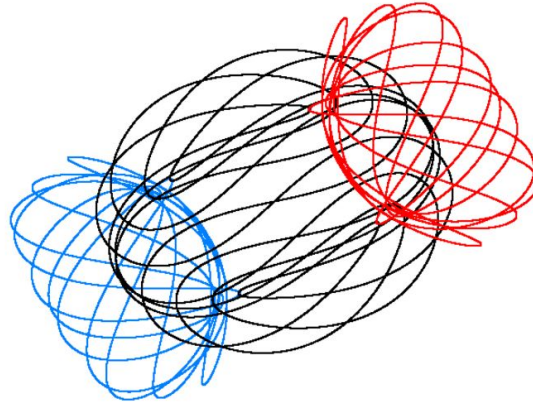


Figure 5: Moth 3 Solution Real Space

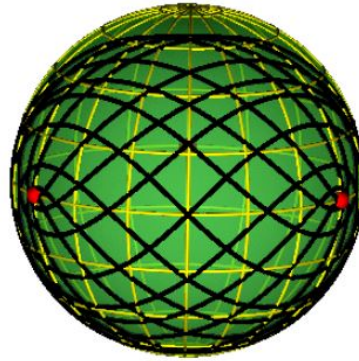


Figure 6: Moth 3 Solution sphere Space

3 respectively where  $p_1=0.383444$ ,  $p_2=0.377364$ , a period of 25.8 and angular momentum zero similarly to the other solutions.

The last solution that will be discussed is a part of the butterfly family of solutions Butterfly IV. This family is named due in large part to its appearance in real space where the center body's path appears to trace out a body of a butterfly and the two outer bodies trace out shapes that resemble wings<sup>7</sup>.

The sphere state of this particular solution is very densely packed around the equator of the sphere space<sup>8</sup>.

This solution also has a mirror symmetry like Goggles, Figure 8, and the Moth family. The conditions for this solution are:  $(p_1, p_2)$ ,  $(p_1, p_2)$ ,  $(-2p_1, -2p_2)$ , where  $p_1=0.350112$  and  $p_2=0.079339$ .

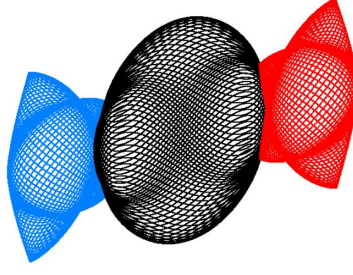


Figure 7: Butterfly IV Solution Real Space

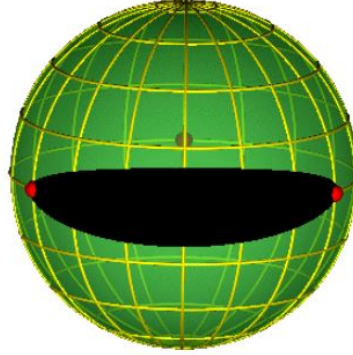


Figure 8: Butterfly IV Solution Sphere Space

This solution has the longest period of those discussed here at 79.5 and still has zero angular momentum.

## 4 Numerical Solution

Since there is no general analytic solution to the 3 body problem, solutions to arbitrary initial conditions must be computed numerically. Several methods have been presented and compared in the following sections. In order to run the simulations on a reasonable time scale for simulation, parameters such as mass,  $G$  and time step  $\Delta t$ . The details of code implementation can be found on the project page.<sup>1</sup>

### 4.1 Runge-Kutta Method (RK4)

The Runge-Kutta method, or RK4, is an iterative method used to numerically solve ODEs. It is a fourth order method that uses an initial function or state  $y_0$  which is incremented in time by computing a slope over a time step  $\Delta t$ . The slope is given by a weighted average of slopes computed at the endpoints and midpoint of the time step.

For the general RK4 method, the initial value problem is set up as:

$$\dot{y} = f(t, y) \quad (19)$$

$$y(t_0) = y_0 \quad (20)$$

For the equations of motion in the 3 body problem, the equation of motion we need to solve is a second-order ODE. Therefore, the equations for a given body become:

$$\dot{\mathbf{y}} = \frac{d\mathbf{v}}{dt} = \frac{d^2\mathbf{r}}{dt^2} = \mathbf{a}(\mathbf{r}_\alpha, \mathbf{r}_\beta, \mathbf{r}_\gamma)|_{t=t_n} \quad (21)$$

$$\mathbf{y}(\mathbf{t}_0) = \mathbf{v}(t_0) = (u(t_0), v(t_0)) \quad (22)$$

The slopes computed by RK4 are  $k_{1,2,3,4}$ , with  $k_1$  computed at the beginning of the timestep,  $k_{2,3}$  computed at the midpoint of the timestep, and  $k_4$  computed at the end of the timestep. The

<sup>1</sup><https://github.com/dma14/Phys350NBody>

positions at which  $f(t, y) = \mathbf{a}$  is calculated for  $k_{i \neq 1}$  depend on the previous  $k$  value. Thus, for a given body  $\alpha$  and time  $t_n = t_0 + n\Delta t$ :

$$\mathbf{k}_1 = f(t_n, \mathbf{y}_n) = \mathbf{a}(\mathbf{r}_\alpha, \mathbf{r}_\beta, \mathbf{r}_\gamma)|_{t=t_n} \quad (23)$$

$$\mathbf{k}_2 = f(t_n + \frac{\Delta t}{2}, \mathbf{y}_n + \mathbf{k}_1 \frac{\Delta t}{2}) = \mathbf{a}(\mathbf{r}_\alpha, \mathbf{r}_\beta, \mathbf{r}_\gamma)|_{t=t_n + \frac{\Delta t}{2}} \quad (24)$$

$$\mathbf{k}_3 = f(t_n + \frac{\Delta t}{2}, \mathbf{y}_n + \mathbf{k}_2 \frac{\Delta t}{2}) = \mathbf{a}(\mathbf{r}_\alpha, \mathbf{r}_\beta, \mathbf{r}_\gamma)|_{t=t_n + \frac{\Delta t}{2}} \quad (25)$$

$$\mathbf{k}_4 = f(t_n + \Delta t, \mathbf{y}_n + \mathbf{k}_3 \Delta t) = \mathbf{a}(\mathbf{r}_\alpha, \mathbf{r}_\beta, \mathbf{r}_\gamma)|_{t=t_n + \Delta t} \quad (26)$$

Note that positions in each step are also implicitly different as the velocities they are incremented over the time step are updated differently.

The final slope of the time step is a weighted average of  $k_{1,2,3,4}$ , with greater weight given to the slopes at the midpoint.

$$\mathbf{y}_{n+1} = \mathbf{y}_n + \frac{1}{6}(\mathbf{k}_1 + 2\mathbf{k}_2 + 2\mathbf{k}_3 + \mathbf{k}_4)\Delta t \quad (27)$$

Therefore, the steps taken in our RK4 implementation for each body are:

1. Compute  $\mathbf{k}_1$  as the initial acceleration at the initial position  $\mathbf{r}_0$ .
2. Increment  $\mathbf{r}_0$  by  $\mathbf{v}_0\Delta t/2$  and  $\mathbf{v}_0$  by  $\mathbf{k}_1\Delta t/2$ . Compute  $\mathbf{k}_2$  as the acceleration at the new position.
3. Increment  $\mathbf{r}_0$  by  $(\mathbf{v}_0 + \mathbf{k}_1\Delta t/2)\Delta t/2$  (the updated velocity of the last step) and  $\mathbf{v}_0$  by  $\mathbf{k}_2\Delta t/2$ . Compute  $\mathbf{k}_3$  as the acceleration at the new position.
4. Increment  $\mathbf{r}_0$  by  $(\mathbf{v}_0 + \mathbf{k}_2\Delta t/2)\Delta t$  and  $\mathbf{v}_0$  by  $\mathbf{k}_3\Delta t$ . Compute  $\mathbf{k}_4$  as the acceleration at the new position.
5. Compute the new state  $(\mathbf{r}_1, \mathbf{v}_1)$  by updating  $(\mathbf{r}_0, \mathbf{v}_0)$  with the weighted average of the velocities and  $\mathbf{k}$  values of the previous steps.

## 4.2 Symplectic Methods

Symplectic integrators are used to numerically solve Hamilton's equations. Since the Hamiltonian for the 3 body problem is separable (i.e. we can write  $H(\mathbf{p}, \mathbf{r}) = T(\mathbf{p}) + V(\mathbf{r})$ ), we can use methods that increment position and velocity independently. An advantage that symplectic integrators have over an RK4 integrator is that the Hamiltonian is conserved (within a bounded error), so the total energy of the simulated system does not drift from the true value over time.

### 4.2.1 Symplectic Euler Method

The Symplectic Euler method is a first order method that is very similar to the standard Euler method, except position and velocity are updated sequentially. Given initial conditions:

$$\mathbf{r}(t_0) = \mathbf{r}_0 \quad (28)$$

$$\mathbf{v}(t_0) = \mathbf{v}_0 \quad (29)$$

New values for  $\mathbf{r}$  and  $\mathbf{v}$  at the next time step are computed as:

$$\mathbf{v}(t + \Delta t) = \mathbf{v}(t) + \frac{d^2\mathbf{r}}{dt^2}\bigg|_{\mathbf{r}(t)} \Delta t \quad (30)$$

$$\mathbf{r}(t + \Delta t) = \mathbf{r}(t) + \mathbf{v}(t + \Delta t)\Delta t \quad (31)$$

### 4.2.2 Velocity Verlet Method

The Velocity Verlet method is a second order symplectic method, which relies on acceleration  $\mathbf{a}(t) = \frac{d^2\mathbf{r}}{dt^2}|_{\mathbf{r}(t)}$  being independent of  $\mathbf{v}(t)$  (which is the case for the equations of motion of the 3 body problem). Then, with the same initial conditions as for the Symplectic Euler method:

$$\mathbf{r}(t + \Delta t) = \mathbf{r}(t) + \mathbf{v}(t)\Delta t + \mathbf{a}(t)\frac{(\Delta t)^2}{2} \quad (32)$$

$$\mathbf{v}(t + \Delta t) = \mathbf{v}(t) + (\mathbf{a}(t) + \mathbf{a}(t + \Delta t))\frac{\Delta t}{2} \quad (33)$$

Note that  $\mathbf{a}(t + \Delta t)$  must be computed using  $\mathbf{r}(t + \Delta t)$  before computing  $\mathbf{v}(t + \Delta t)$ .

### 4.3 Error Analysis

The three numerical methods mentioned in the previous subsection have an error dependent upon the  $\Delta t$  chosen for the iteration of the solution. The choice for the  $\Delta t$  was a compromise between efficiency and accuracy. With a smaller time step the accuracy of the solution increases, but computation time also increases. After comparing the results of different time steps based on accuracy and computation time we would recommend a time step of  $10^{-2}$  for the simulation for accuracy. However, for the public version of our code we implemented a  $\Delta t$  of 1 to ensure that the simulation would run at a reasonable rate.

Figure 9 shows a plot of the Y velocity of Object 1 with the three numerical methods we have discussed previously: RK4, Symplectic Euler Method, and the Velocity Verlet Method. Figure 10 shows the absolute difference between the methods.<sup>2</sup> Figure 10 shows that RK4 and velocity verlet yield extremely similar results, However, the overall difference between the three methods is very small, with the most variance in solution appearing where the velocity of the object is small, which is as expected, since when the velocities are small the errors due to time-step and rounding are magnified.

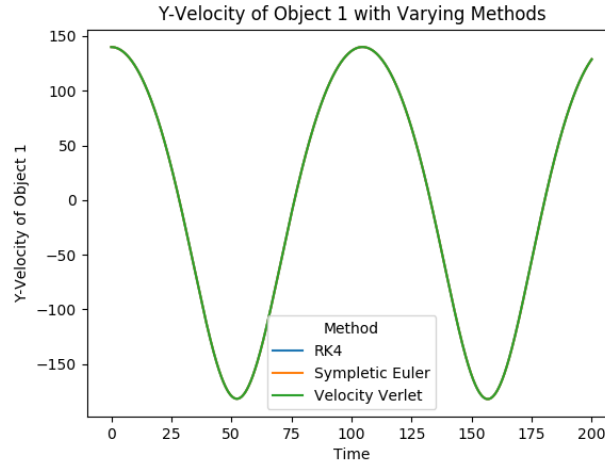


Figure 9: Y-Velocity of Object 1 simulated with various methods with a  $\Delta t$  of  $10^{-2}$

From Figures 11, 12, and 13 it is clear that no method clearly stands out in terms of accuracy. All three methods converge linearly and the difference between the errors with each convergence are very similar, to the point where it is negligible. Although it is normal for symplectic integrators to have a linearly decreasing error, the RK4 method is of accuracy  $O(h^4)$ , which is not seen in the graphs. Unfortunately, we were unable to determine the source of this error in our integrator. The simulation decreases with accuracy over time as most of the errors are cumulative, and increases with accuracy with a decrease in  $\Delta t$ .

<sup>2</sup>Figures 9, 10, 11, 12, and 13 all show the Y velocity of Object 1 in a simulation with initial conditions of: Object 1 at  $[3e3, 0e3]$  with velocity  $[0, 140]$  and mass 1; Object 2 at  $[0, 0]$  with velocity  $[0, 0]$  and mass 1; Object 3 at  $[-3e3, 0]$  and velocity  $[0, -140]$  and mass 1.



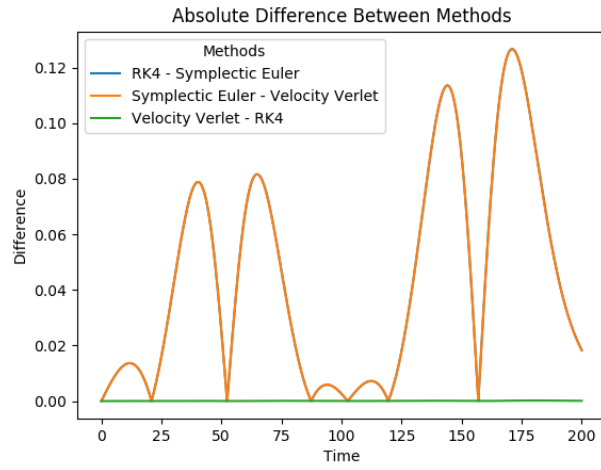


Figure 10: Difference between the various methods

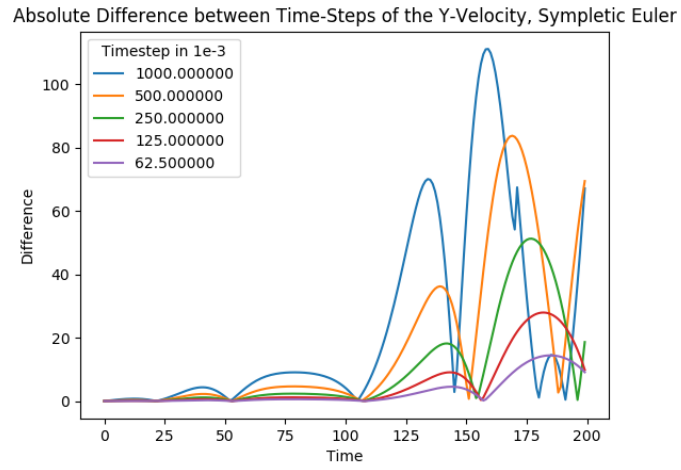


Figure 11: Absolute difference between time steps in the Symplectic Euler integrator

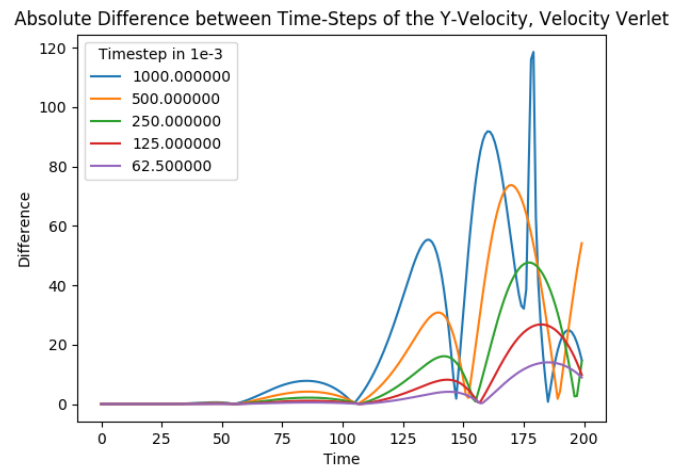


Figure 12: Absolute difference between time steps in the Velocity Verlet integrator

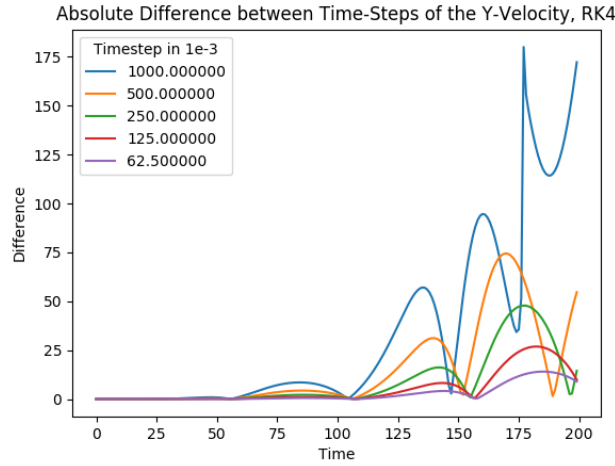


Figure 13: Absolute difference between time steps in the RK4 integrator

## 5 Program Features

Our final simulation code can be found at <https://github.com/dma14/Phys350NBody>. The simulation uses the python libraries [matplotlib](#) and [numpy](#) to model a 3-body system in 2D and 3D<sup>3</sup>. Through a simple GUI<sup>14</sup>, it allows the user to set the initial conditions of the system: the mass, velocity, and position of the three bodies, as well as selecting from some preset initial conditions. The simulation code has functionality for using RK4, Euler, or Velocity Verlet integration methods, with Velocity Verlet being set as default. The figure below shows sample 2D<sup>15</sup> and 3D<sup>16</sup> plots of our simulation with similar ICs.

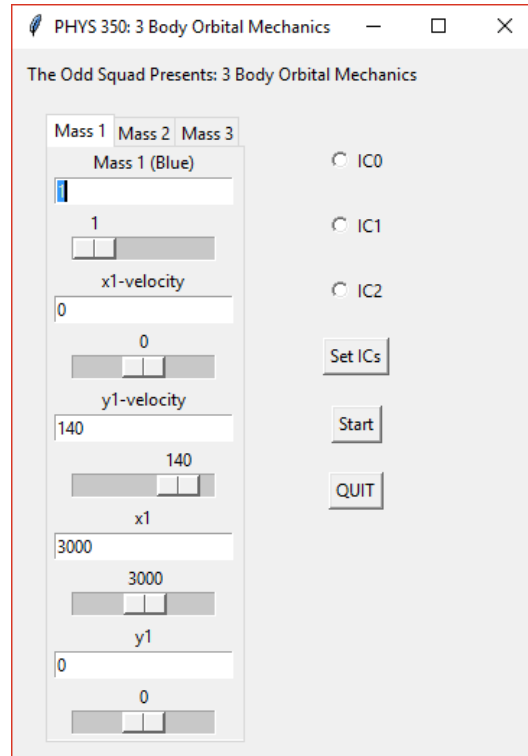


Figure 14: Simulation GUI

<sup>3</sup>For implementation efficiency, the 2D and 3D simulators have been split up between the "master" and "3dAnim" branches on the GitHub repository.

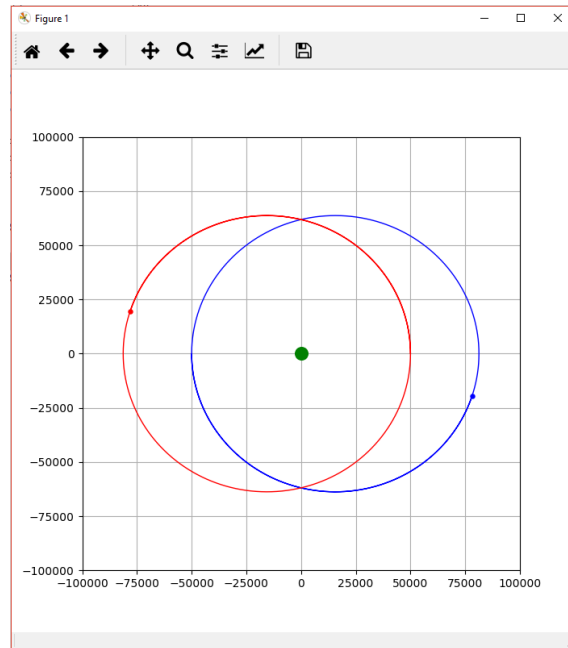


Figure 15: Sample 2D plot

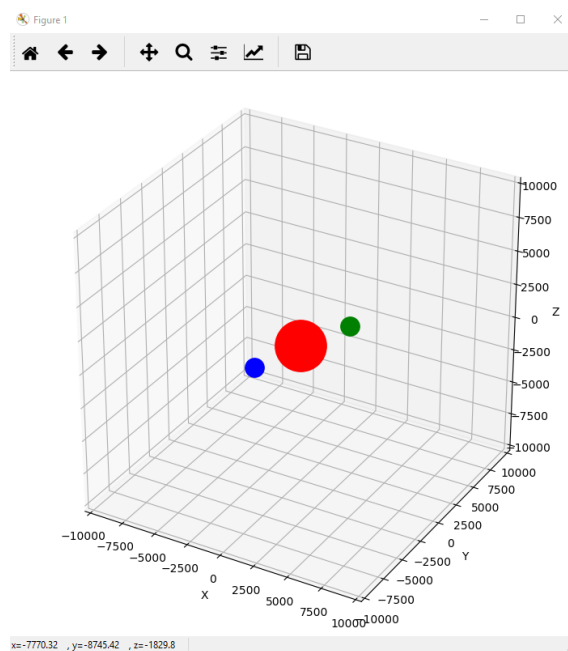


Figure 16: Sample 3D plot

## References

- [Bro75] R. Broucke. On relative periodic solutions of the planar general three-body problem. *Celestial Mechanics*, 12(4):439–462, 1975.
- [CM00] Alain Chenciner and Richard Montgomery. A remarkable periodic solution of the three-body problem in the case of equal masses. *The Annals of Mathematics*, 152(3):881, Nov 2000.
- [Hen74] M. Henon. Families of periodic orbits in the three-body problem. *Celestial Mechanics*, 10(3):375–388, 1974.
- [HEN76] M. HENon. A family of periodic solutions of the planar three-body problem, and their stability. *Celestial Mechanics*, 13(3):267–285, May 1976.
- [Moo93] Cristopher Moore. Braids in classical dynamics. *Physical Review Letters*, 70(24):3675–3679, Jun 1993.
- [SD13] Milovan Suvakov and V. Dmitrasinovic. Three classes of newtonian three-body planar periodic orbits. *Physical Review Letters*, 110(11), 2013.